ANTIOXIDANTS & REDOX SIGNALING
Volume 22, Number 15, 2015

DOI: 10.1089/ars.2014.6004

Discoveries

ORIGINAL RESEARCH COMMUNICATION

Autophagy Attenuates Noise-Induced Hearing Loss by Reducing Oxidative Stress

Hu Yuan,[1,*] Xianren Wang,[1] Kayla Hill,[1] Jun Chen,[1] John Lemasters,[2] Shi-Ming Yang,[3] and Su-Hua Sha[1]

Abstract

Aims: Reactive oxygen species play a dual role in mediating both cell stress and defense pathways. Here, we used pharmacological manipulations and siRNA silencing to investigate the relationship between autophagy and oxidative stress under conditions of noise-induced temporary, permanent, and severe permanent auditory threshold shifts (temporary threshold shift [TTS], permanent threshold shift [PTS], and severe PTS [sPTS], respectively) in adult CBA/J mice. ***Results:*** Levels of oxidative stress markers (4-hydroxynonenal [4-HNE] and 3-nitrotyrosine [3-NT]) increased in outer hair cells (OHCs) in a noise-dose-dependent manner, whereas levels of the autophagy marker microtubule-associated protein light chain 3 B (LC3B) were sharply elevated after TTS but rose only slightly in response to PTS and were unaltered by sPTS noise. Furthermore, green fluorescent protein (GFP) intensity increased in GFP-LC3 mice after TTS-noise exposure. Treatment with rapamycin, an autophagy activator, significantly increased LC3B expression, while diminishing 4-HNE and 3-NT levels, reducing noise-induced hair cell loss, and, subsequently, noise-induced hearing loss (NIHL). In contrast, treatment with either the autophagy inhibitor 3-methyladenine (3MA) or LC3B siRNA reduced LC3B expression, increased 3-NT and 4-HNE levels, and exacerbated TTS to PTS. ***Innovation:*** This study demonstrates a relationship between oxidative stress and autophagy in OHCs and reveals that autophagy is an intrinsic cellular process that protects against NIHL by attenuating oxidative stress. ***Conclusions:*** The results suggest that the lower levels of oxidative stress incurred by TTS-noise exposure induce autophagy, which promotes OHC survival. However, excessive oxidative stress under sPTS-noise conditions overwhelms the beneficial potential of autophagy in OHCs and leads to OHC death and NIHL. *Antioxid. Redox Signal.* 22, 1308–1324.

Introduction

A KEY ELEMENT CONTRIBUTING TO noise-induced hearing loss (NIHL) is oxidative damage to sensory hair cells. Oxidative stress is designated as an imbalance between the production of reactive oxygen species (ROS) and antioxidant defenses, potentially resulting in oxidative damage (45). Oxidative damage can be caused by increased ROS production without an increase in antioxidant activity or by decreased antioxidant activity without an increase in ROS, or a combination of the two. Overproduction of ROS and reactive nitrogen species (RNS) has emerged as a common pathologic mechanism of various inner ear insults, such as noise exposure and ototoxic drug treatment, including in cochlear tissues (52) and fluids (35). ROS are molecules or ions formed by the incomplete single-electron reduction of oxygen. These reactive oxygen intermediates include singlet oxygen, superoxide, peroxides, hydroxyl radicals, and hypochlorous acid. RNS are nitric oxide-derived compounds and include nitroxyl anion, nitrosonium cation, higher oxides of nitrogen, S-nitrosothiols, and dinitrosyl iron complexes (11, 26). Markers of oxidative stress, as indicated by products of lipid oxidation (4-hydroxynonenal [4-HNE]) and protein nitration (3-nitrotyrosine [3-NT]), increase in sensory hair cells after noise exposure, including in outer hair cells (OHCs) (53). Antioxidant defense mechanisms increase transiently in response to the inner ear stress and then decrease with prolonged insults (7). In addition, a causal relationship between

Departments of [1]Pathology and Laboratory Medicine and [2]Biochemistry and Molecular and Pharmaceutical Sciences, Medical University of South Carolina, Charleston, South Carolina.
[3]Department of Otolaryngology-Head and Neck Surgery, Chinese PLA General Hospital, Beijing, People's Republic of China.
Current affiliation: Department of Otolaryngology-Head and Neck Surgery, Chinese PLA General Hospital, Beijing, People's Republic of China.

Innovation

Reactive oxygen species (ROS) not only are well known to induce outer hair cell death but also have been shown to play a dual role in sensory hair cells under different noise exposure conditions. Temporary threshold shift noise induces low levels of oxidative stress, activating the autophagy process, while severe permanent threshold shift noise induces excessive oxidative stress, resulting in oxidative damage. This study demonstrates a relationship between oxidative stress and autophagy in sensory hair cells and reveals that autophagy is an intrinsic cellular process that attenuates noise-induced hearing loss (NIHL) by reducing oxidative stress. This novel finding thus supports, *via* an independent approach, the notion of a causal relationship between ROS and NIHL.

oxidative damage and NIHL is supported by evidence that antioxidants given before or shortly after noise exposure attenuate noise-induced hair cell death and NIHL (10, 16, 53).

ROS also have the ability to induce cellular defense pathways such as autophagy (48), a protective process that delivers damaged cellular components to lysosomes for degradation (50). This process is mediated *via* the formation of autophagosomes (2, 12) that fuse with lysosomes to enzymatically degrade the engulfed components (33). The orderly disposal of these potentially damaged cellular constituents, including impaired organelles and misfolded proteins, plays a protective role limiting pathological alterations (4, 41). In neuronal cells, the activation of autophagy ameliorates brain injury and cortical neuron apoptosis (51). The pharmacological upregulation of autophagy increases the number of surviving retinal ganglion cells, while the deletion of autophagy genes reduces cell survival during optic nerve degeneration (42). Microtubule-associated light chain 3 protein (LC3) is an essential component associated with the autophagosome membrane and is involved in the mechanism of autophagy at a molecular level. In humans, three genes encode highly homologous LC3 proteins (LC3A, B, and C), two of which (LC3A and LC3B) are conserved in mice. The splicing variant LC3B has the broadest specificity and acts as a suitable marker for autophagy activity in cells (1).

Although the complex relationship of autophagy with ROS levels suggests a potential role for autophagy in NIHL, this has yet to be established. We hypothesize that lower levels of oxidative stress, as seen with temporary threshold shifts (TTS), stimulate autophagy, protecting against NIHL, while excessive oxidative stress induces oxidative damage in OHCs, leading to permanent threshold shifts (PTS). To investigate this hypothesis, we first characterized noise-exposure conditions for TTS, PTS, and severe PTS (sPTS) in male CBA/J mice at 3 months of age. We then assessed oxidative stress as indicated by products of lipid oxidation and protein nitration and the expression of the autophagy marker LC3B in OHCs under these three noise conditions. Healthy transgenic mice systemically expressing green fluorescent protein (GFP) fused to LC3 (a mammalian homologue of yeast Atg8) were generated (23, 32). We used GFP-LC3 mice to confirm the augmentations of cellular autophagy after TTS noise. The relationship between autophagy and oxidative stress, as well as auditory thresholds, was further explored using siRNA silencing and pharmacological modulators, specifically the autophagy activator rapamycin and the autophagy inhibitor 3-methyladenine (3MA).

Results

Noise exposures induce temporary and permanent hearing loss in adult CBA/J mice

Previous studies by our laboratory demonstrated that exposure of 12-week-old male CBA/J mice for 2 h to 2–20 kHz broadband noise (BBN) at 92, 94, or 96 dB SPL induces TTS, while intensities of 98, 100, 102, 104, and 106 dB SPL result in hair cell death and PTS without altering supporting cell and spiral ganglion cell structure as per light microscopy evaluation (6). In this study, we characterized the effects of noise exposure at 96, 98, and 106 dB SPL in detail.

Exposure to BBN at 96 dB SPL for 2 h resulted in significant auditory threshold shifts of 20, 50, and 50 dB at 8, 16, and 32 kHz, respectively, 3 h postexposure ($F_{2,90} = 101.377$, $p < 0.001$). The auditory thresholds measured by auditory brainstem response (ABR) at all three frequencies partially recovered 1 day after the exposure with full recovery by 3 days after exposure, confirming that the noise condition leads to TTS only ($F_{3,45} = 33.633$, $p < 0.001$) (Fig. 1A). Exposures at 98 dB SPL created significant threshold shifts of 30, 50, and 55 dB at 8, 16, and 32 kHz, respectively, at 3 days after the exposure ($F_{2,112} = 213.382$, $p < 0.001$), which remained stable for 7 to 14 days at 16 and 32 kHz, but recovered partially at 8 kHz ($F_{2,56} = 1.857$, $p = 0.166$) (Fig. 1B). Exposure to 106 dB SPL resulted in even larger threshold shifts at 8, 16, and 32 kHz at 3 days after exposure ($F_{2,98} = 150.876$, $p < 0.001$) that remained stable for 7 to 14 days at all three frequencies ($F_{2,49} = 0.415$, $p = 0.663$) (Fig. 1C). Detailed *post-hoc* tests for comparison of auditory threshold shifts from all three noise conditions are listed in Table 1. Two weeks after noise exposure, hair cell loss was quantified for all three conditions. There were no OHC or inner hair cell (IHC) losses after 96-dB TTS noise (Fig. 1D). The 98-dB SPL exposure resulted in OHC losses only, beginning around 3.5 mm from the apex and increasing toward the base, while IHCs remained intact (Fig. 1E, F). The 106-dB SPL noise exposure resulted in losses of both OHCs and IHCs. OHC losses began around 2.5 mm from the apex and IHC losses began around 4.5 mm from the apex, and both increased as a function of distance from the apex (Fig. 1E, F). The amount of OHC loss induced by 106 dB SPL was significantly higher than by 98 dB SPL ($F_{1,8} = 189{,}986$, $p < 0.001$, Fig. 1E). We therefore refer to the 98 dB SPL noise conditions as ''PTS noise'' and the 106 dB SPL noise conditions as severe, or ''sPTS noise.'' Age-matched sham-exposed control mice showed no elevation of auditory thresholds 2 weeks after exposure.

Noise-induced elevations of 3-NT and 4-HNE levels in OHCs are noise-dose dependent

Increased oxidative stress, as indicated by products of lipid oxidation, and protein nitration, determined by increased 4-HNE and 3-NT levels, have been well documented after noise exposure (53). We first assessed 3-NT and 4-HNE levels under control conditions without noise exposure and PTS-noise conditions in whole cochlear tissue homogenates

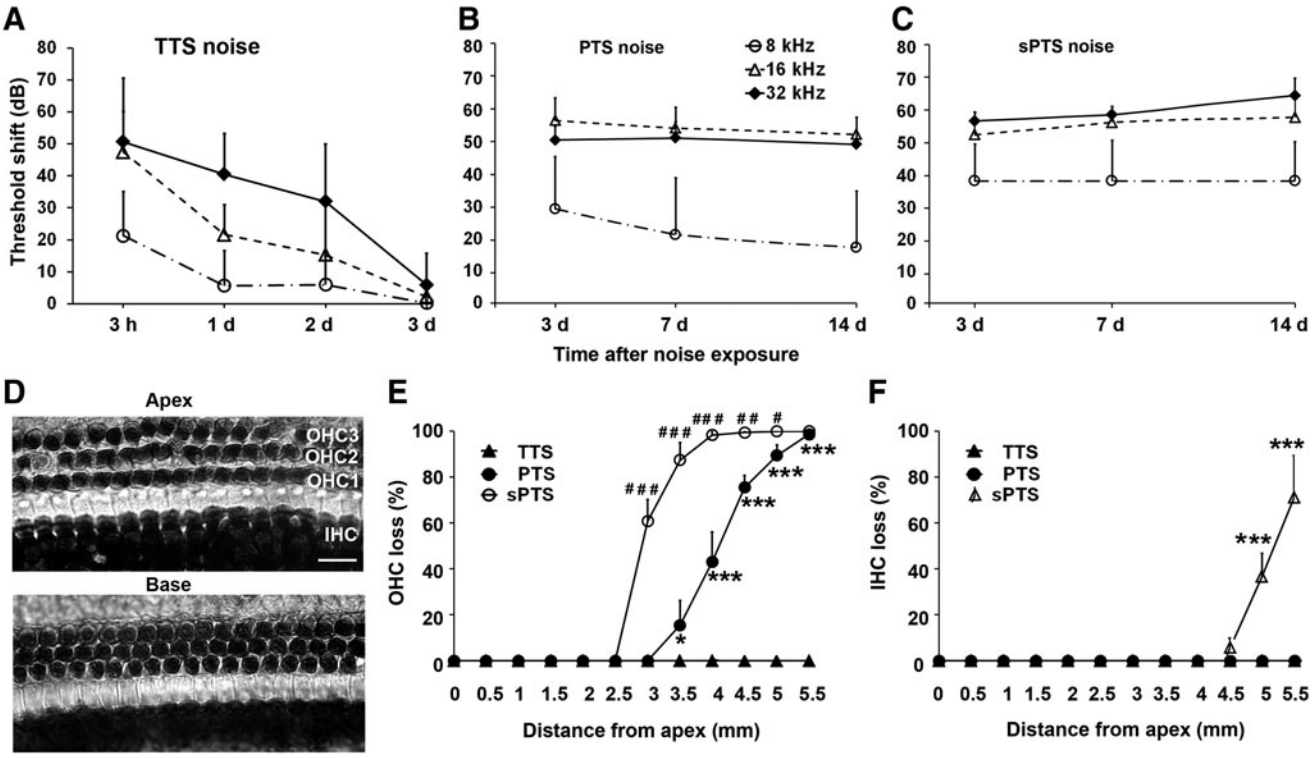

FIG. 1. Noise induces TTS, PTS, and sPTS in adult CBA/J mice. **(A)** TTS: 96 dB SPL induces significant threshold shifts at 8, 16, and 32 kHz 3 h after exposure with complete recovery by day 3. Three hours: $n=8$, 1 day: $n=14$, 2 days: $n=7$, 3 days: $n=20$ mice. **(B)** PTS: 98 dB SPL induces significant threshold shifts at 8, 16, and 32 kHz 3 days after noise exposure that are maintained through 14 days. Three days: $n=16$, 7 days: $n=18$, 14 days: $n=25$ mice. **(C)** sPTS noise: 106-dB SPL noise significantly increases thresholds at 8, 16, and 32 kHz 3 days after noise exposure that are maintained through 14 days. Three days: $n=8$, 7 days: $n=19$, 14 days: $n=25$ mice. **(D)** Representative images of myosin-VII-labeled and then DAB-stained surface preparations for hair cell counts in the apex and base show no OHC or IHC loss 3 days after TTS-noise exposure. Scale bar = 10 μm. **(E)** Quantification of OHC losses 14 days after noise exposure revealed significantly more OHC loss with sPTS *versus* PTS and no OHC loss under TTS conditions. $^{\#}$ or $^{*}p<0.05$, $^{\#\#}p<0.01$, $^{\#\#\#}$ or $^{***}p<0.001$ ($^{\#}$sPTS *vs.* PTS, *PTS *vs.* TTS). **(F)** sPTS noise also results in IHC losses in the basal turn. $^{***}p<0.001$, $n=5$. Data **(A–C, E, F)** are presented as means + SD. DAB, diaminobenzidine; IHC, inner hair cell; OHCs, outer hair cells; PTS, permanent threshold shift; sPTS, severe PTS; TTS, temporary threshold shift.

by Western blot. In agreement with a previous report, incubation with 3-NT and 4-HNE antibodies each revealed a 70-kDa band (18). The 3-NT band density increased significantly 1 h after PTS-noise exposure compared with controls ($t_3=4.805$, $p=0.017$) (Fig. 2B). However, the levels of 4-HNE were unchanged (Fig. 2D). Next, we analyzed the expression of 3-NT and 4-HNE on surface preparations 1 h after exposure to the three noise conditions. Immunolabeling of both 3-NT and 4-HNE increased in OHCs and supporting cells compared with controls (Fig. 2A, C). Quantitative analysis of 3-NT immunolabeling in OHCs revealed that sPTS noise induces a 100% increase ($t_2=8.660$, $p=0.013$), PTS induces a 70% increase ($t_2=8.111$, $p=0.015$), and TTS induces a marginal 20% increase, relative to age-matched controls without noise exposure ($t_2=4.305$, $p=0.050$) (Fig. 2A′). Quantitative analysis of 4-HNE immunolabeling in OHCs also showed a 150% increase after sPTS ($t_5=2.911$, $p=0.03$) and a 100% increase after PTS ($t_5=3.861$, $p=0.012$), but not after TTS-noise exposure ($t_5=1.998$, $p=0.102$) compared with controls (Fig. 2C′). Furthermore, treatment with the antioxidant N-acetylcysteine (NAC) reduced PTS-noise-induced immunolabeling of 3-NT levels by 40% ($t_2=-8.246$, $p=0.014$) and of 4-HNE levels by 90% in OHCs ($t_2=-62.794$, $p<0.001$) (Fig. 3A, A′ for 3-NT; Fig. 3B, B′ for 4-HNE).

Moderate noise induces increased formation of autophagosomes in OHCs

First, the levels of autophagosome marker LC3B were assessed in whole cochlear tissue homogenates by Western blot. LC3B band densities at both 16 kDa (LC3B-I) and 14 kDa (LC3B-II) were unchanged after TTS-noise exposure compared with age-matched controls (Fig. 4E). Next, we evaluated the autophagosome marker LC3B in sensory hair cells in response to TTS-, PTS-, and sPTS-noise treatment compared with age-matched control mice. LC3B immunofluorescence showed a punctuate pattern in OHCs (Fig. 4A, enlarged images) that was stronger 1 h after TTS-noise exposure compared with PTS and control preparations (Fig. 4A, panels: control, TTS noise 1 h, PTS noise 1 h). Quantitative analysis of LC3B immunolabeling in OHCs confirmed a statistically significant increase for both TTS- ($t_3=14.679$, $p<0.001$) and PTS-noise conditions ($t_4=5.570$, $p=0.005$),

Table 1. *Post-hoc* Testing Shows Statistical Values for Each Comparison of Auditory Threshold Shifts Under the Three Noise Conditions Presented in Figures 1A–C

		Post-hoc *test*		
Noise (dB SPL)	*Postnoise*	*Frequency (kHz)*	F-*value*	p-*Value*
TTS-96	3 h	8 *vs.* 16	$F_{1,44} = 96.06$	< 0.001
		8 *vs.* 32	$F_{1,44} = 41.91$	< 0.001
		16 *vs.* 32	$F_{1,44} = 0.47$	0.5
	1 day	8 *vs.*16	$F_{1,44} = 55.782$	< 0.001
		8 *vs.* 32	$F_{1,44} = 91.655$	< 0.001
		16 *vs.* 32	$F_{1,44} = 26.57$	< 0.001
	2 days	8 *vs.* 16	$F_{1,44} = 12.2$	< 0.001
		8 *vs.* 32	$F_{1,44} = 30.33$	< 0.001
		16 *vs.* 32	$F_{1,44} = 11.82$	0.001
	3 days	8 *vs.* 16	$F_{1,44} = 2.01$	0.164
		8 *vs.* 32	$F_{1,44} = 4.97$	0.031
		16 *vs.* 32	$F_{1,44} = 1.94$	0.171
PTS-98	3 days	8 *vs.* 16	$F_{1,56} = 68.6$	< 0.001
		8 *vs.* 32	$F_{1,56} = 49.87$	< 0.001
		16 *vs.* 32	$F_{1,56} = 6.11$	0.017
	7 days	8 *vs.* 16	$F_{1,56} = 77.17$	< 0.001
		8 *vs.* 32	$F_{1,56} = 60.14$	< 0.001
		16 *vs.* 32	$F_{1,56} = 3.89$	0.054
	14 days	8 *vs.* 16	$F_{1,56} = 130.05$	< 0.001
		8 *vs.* 32	$F_{1,56} = 104.93$	< 0.001
		16 *vs.* 32	$F_{1,56} = 4.53$	0.038
sPTS-106	3 days	8 *vs.* 16	$F_{1,49} = 33.37$	< 0.001
		8 *vs.* 32	$F_{1,49} = 42.98$	< 0.001
		16 *vs.* 32	$F_{1,49} = 4.68$	0.035
	7 days	8 *vs.* 16	$F_{1,49} = 82.58$	< 0.001
		8 *vs.* 32	$F_{1,49} = 98.52$	< 0.001
		16 *vs.* 32	$F_{1,49} = 8.56$	0.005
	14 days	8 *vs.* 16	$F_{1,49} = 102.02$	< 0.001
		8 *vs.* 32	$F_{1,49} = 133.11$	< 0.001
		16 *vs.* 32	$F_{1,49} = 15.03$	< 0.001

PTS, permanent threshold shift; sPTS, severe PTS; TTS, temporary threshold shift.

but not for sPTS ($t_4 = 2.075$, $p = 0.107$), with significantly higher fluorescence intensity under TTS (2.3 times control) than PTS conditions (1.5 times control) ($t_8 = 9.349$, $p < 0.001$) (Fig. 4B).

We then examined the effects of 3MA, an autophagy inhibitor, and rapamycin, an autophagy activator, on autophagosome formation in response to noise exposure. Since levels of LC3B were greater after TTS than after PTS noise, the TTS condition was used to examine the possible blocking effect of the autophagosome inhibitor 3MA, while the PTS condition was exploited to assess potential rapamycin-mediated elevation of LC3B. Surface preparations showed a decrease in LC3B immunolabeling in OHCs of TTS-noise-exposed mice treated with 3MA compared with mice exposed to TTS noise only (Fig. 4A, panels: TTS noise + 3MA 1 h, TTS noise 1 h). In contrast, rapamycin treatment potentiated the induction of LC3B by PTS noise in OHCs (Fig. 4A, panels: PTS noise + rapamycin [RAP] 1 h, PTS noise 1 h). Quantitative analysis of LC3B-associated immunofluorescence confirmed that the reduction in intensity by 3MA treatment in TTS was about 40% ($t_7 = 8.957$, $p < 0.001$) (Fig. 4C) and enhancement of intensity by rapamycin treatment in PTS was 25% ($t_{12} = 5.584$, $p < 0.001$) (Fig. 4D). The administration of 3MA alone did not influence the levels of LC3B ($t_2 = 0.962$, $p = 0.055$) nor did vehicle (dimethyl sulfoxide [DMSO]) alone ($t_2 = 0.693$, $p = 0.561$). In contrast, the administration of rapamycin alone increased levels of LC3B compared with controls ($t_3 = 9.708$, $p = 0.002$), although levels did not reach those achieved by rapamycin with PTS-noise exposure (Fig. 4D).

To confirm the increase in autophagy after noise exposure, we used GFP-LC3 mice. Five-week-old GFP-LC3 mice were exposed to 90-dB SPL noise, resulting in TTS (data not shown). Surface preparations showed that punctuate GFP fluorescence in OHCs (Fig. 5A, enlarged images) was much greater 1 h after the noise exposure compared with age-matched GFP-LC3 littermates not exposed to noise (Fig. 5A). Quantification of GFP fluorescence revealed a ratio of 1:2.5 for controls *versus* TTS-noise-exposed mice ($t_3 = 9.255$, $p = 0.003$) (Fig. 5A′).

TTS-noise exposure induces formation of autolysosomes in OHCs

The formation of autophagosome/lysosome complexes (autolysosomes) was assessed by analyzing the co-localization of the autophagosome marker LC3B with the lysosome marker LAMP1 on surface preparations. Because TTS conditions induce a marked increase in LC3B immunolabeling, the co-localization of LC3B and lysosome marker LAMP1 in OHCs was analyzed 1 h after TTS noise. LAMP1 immunolabeling did not change after TTS noise, but co-localization of LC3B and LAMP1 fluorophores was increased in OHCs (Fig. 6A). Quantification of the overlap coefficient for LC3B/LAMP1 fluorophores using Zeiss Zen software from original confocal images showed a 23% increase in autolysosome abundance in OHCs after TTS noise ($t_{10} = 7.246$, $p < 0.001$) (Fig. 6A′).

Potentiation of autophagy attenuates oxidative stress in OHCs

To determine the relationship of autophagy with oxidative stress, we first assessed the effects of the pharmacological autophagy inhibitor 3MA on 3-NT and 4-HNE levels in OHCs. Treatment with the autophagy inhibitor 3MA markedly increased TTS-noise-induced 3-NT and 4-HNE immunolabeling in OHCs and Deiters cells compared with TTS noise alone (Fig. 7A, B, panels: TTS noise 1 h, TTS noise + 3MA 1 h). Quantification of 3-NT and 4-HNE immunolabeling in OHCs 1 h after TTS-noise exposure confirmed significant increases with 3MA treatment compared with saline controls (3-NT, $t_4 = 4.478$, $p = 0.011$; 4-HNE, $t_2 = 6.543$, $p = 0.023$) (Fig. 7A′, B′). We then assessed the effects of increased autophagy on 3-NT and 4-HNE levels using the pharmacological autophagy stimulator rapamycin. Treatment with rapamycin markedly reduced 3-NT and 4-HNE immunolabeling in OHCs in PTS-noise-exposed cochleae 1 h after the exposure (Fig. 7C, D, panels: PTS noise, PTS noise + RAP 1 h). Quantification of 3-NT and 4-HNE immunolabeling in OHCs confirmed significant attenuation of the PTS-noise-increased 3-NT levels ($t_7 = 3.632$, $p = 0.008$) (Fig. 7C′) and 4-HNE levels ($t_6 = 2.960$, $p = 0.026$) (Fig. 7D′) after treatment with rapamycin. Treatment with DMSO, the

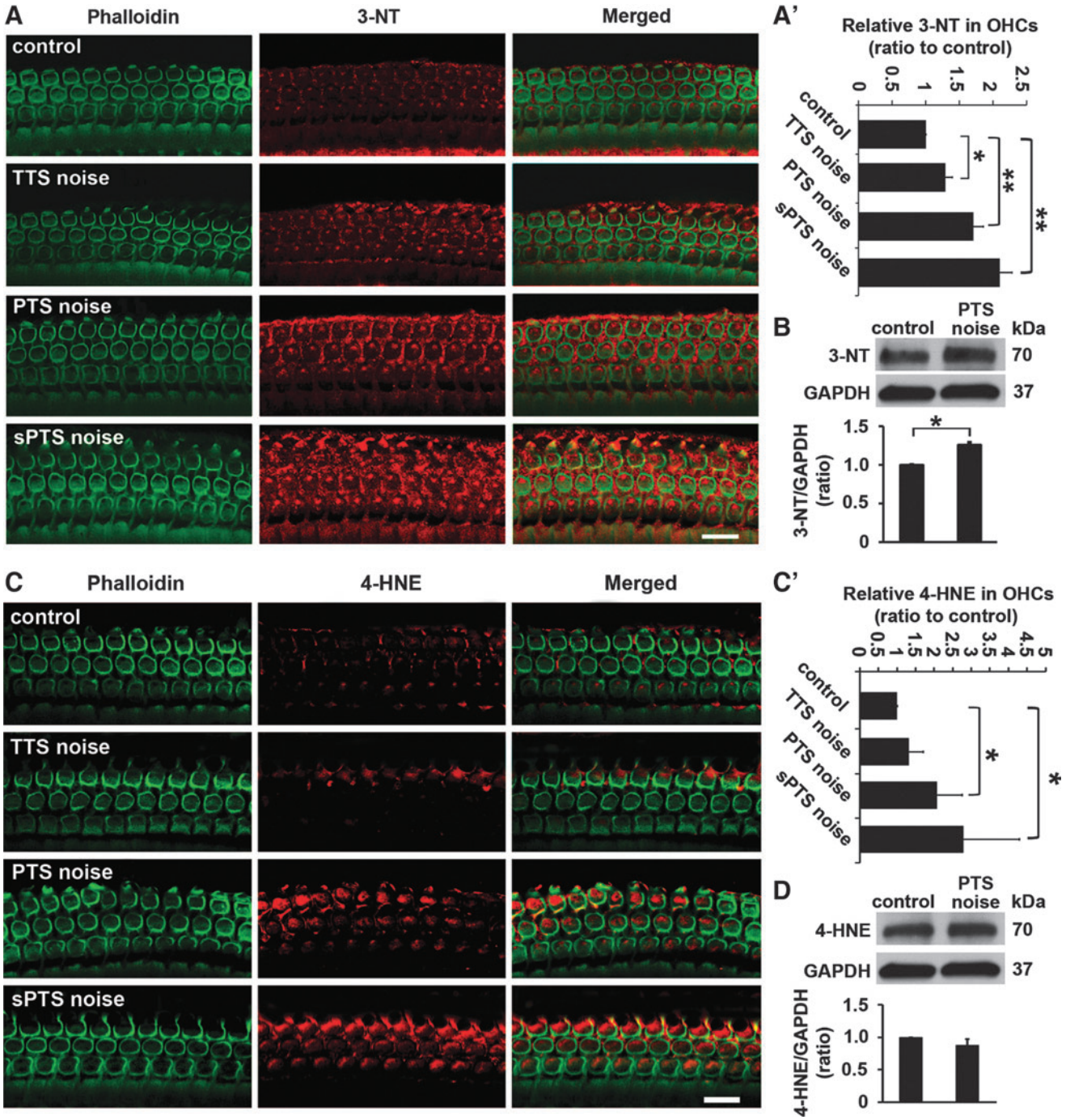

FIG. 2. Noise exposure alters the expression of 3-NT and 4-NHE levels in OHCs. (A) Immunolabeled 3-NT (*red*) in OHCs with phalloidin staining (*green*) 1 h after TTS-, PTS-, and sPTS-noise conditions was stronger than control mice without noise exposure. $n = 3$. **(A′)** Quantification of 3-NT immunolabeling in OHCs showed significant increases in a noise-dose-dependent fashion. $n = 3$. **(B)** Immunoblots labeled with 3-NT antibody revealed that the ratio of the 3-NT band density between control and PTS-exposed mice is significantly different. $n = 4$. **(C)** Immunolabeled 4-HNE (*red*) in OHCs with phalloidin staining (*green*) 1 h after TTS-, PTS-, and sPTS-noise conditions was greater than control mice without noise exposure. $n = 6$. **(C′)** Quantification of 4-HNE immunolabeling in OHCs showed significant increases in a noise-dose-dependent fashion. $n = 6$. **(D)** Immunoblots labeled with 4-HNE antibody revealed that the ratios of 4-HNE band density to GAPDH in control and PTS-exposed mice are similar. $n = 3$. GAPDH serves as the sample loading control in **(B, D)**. Representative images **(A, C)** were taken from the basal turn, scale bar = 10 μm. Data **(A′, B, C′, D)** are presented as means + SD, $*p < 0.05$, $**p < 0.01$. 3-NT, 3-nitrotyrosine; 4-HNE, 4-hydroxynonenal. To see this illustration in color, the reader is referred to the web version of this article at www.liebertpub.com/ars

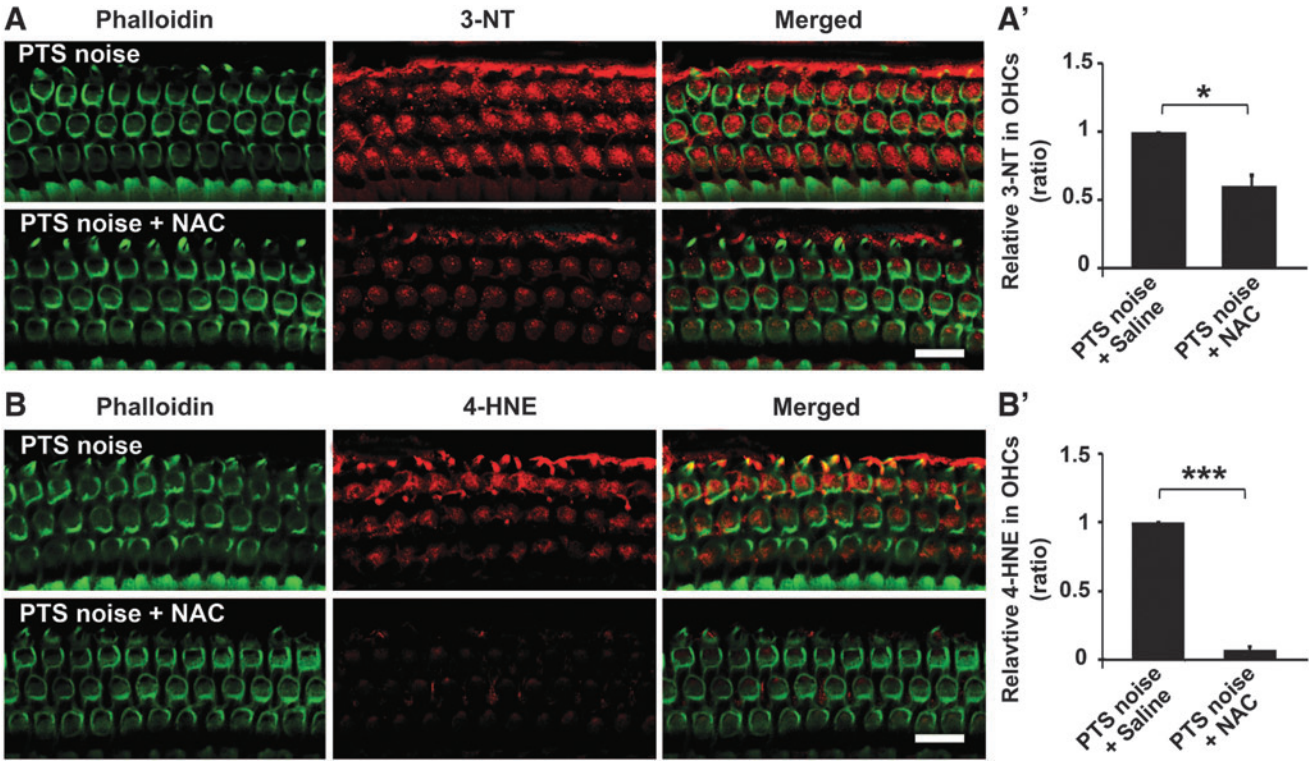

FIG. 3. Antioxidant (NAC) treatment reduces the PTS-noise-increased 3-NT and 4-HNE levels in OHCs. (A) Immunolabeling of 3-NT (*red*) in OHCs with phalloidin staining (*green*) was weak with NAC treatment 1 h after PTS-noise exposure. $n=3$. **(A′)** Quantification of 3-NT immunolabeling in OHCs confirmed a significant decrease with NAC treatment. $n=3$. **(B)** Immunolabeled 4-HNE (*red*) in OHCs with phalloidin staining (*green*) was also reduced with NAC treatment 1 h after PTS-noise exposure. $n=3$. **(B′)** Quantification of 4-HNE immunolabeling in OHCs confirmed a significant reduction with NAC treatment. $n=3$. Representative images **(A, B)** were taken from the basal turn, scale bar = 10 μm. Data **(A′, B′)** are presented as means + SD; $*p<0.05$, $***p<0.001$. NAC, N-acetylcysteine. To see this illustration in color, the reader is referred to the web version of this article at www.liebertpub.com/ars

vehicle control of rapamycin, altered neither 3-NT nor 4-HNE levels in OHCs.

Finally, we assessed the ability of LC3B siRNA (siLC3B) to decrease autophagosome formation under TTS-noise conditions. siLC3B was delivered locally to the round window (7, 37). Two concentrations of siLC3B, 0.3 and 0.6 μg, were tested. Surface preparations showed a significant reduction of around 30% in LC3B expression in OHCs at 72 h after pretreatment with 0.6 μg siLC3B compared with treatment with scrambled siRNA (siControl) ($t_2=5.5120$, $p=0.0314$) (Fig. 8A, A′). Exposure of siLC3B-pretreated mice to TTS noise resulted in a 40% reduction in LC3B levels in OHCs relative to siControl-treated mice 1 h after the exposure ($t_5=8.666$, $p<0.001$) (Fig. 8B, B′).

In addition, pretreatment with siLC3B resulted in increased immunolabeling of both 3-NT and 4-HNE in OHCs compared with siControls 1 h after TTS noise (Fig. 8C, D). Levels of 3-NT and 4-HNE immunolabeling in OHCs of siLC3B-treated cochleae were significantly higher than in siControls (3-NT, $t_4=3.981$, $p=0.0164$; 4-HNE, $t_2=21.683$, $p=0.002$) (Fig. 8C′, D′).

Manipulation of autophagy modulates the magnitude of NIHL and hair cell death

The preceding experiments showed that exposure to the pharmacological regulators 3MA and rapamycin, as well as LC3B siRNA, alters noise-induced autophagosome formation in OHCs. Here, we addressed the questions of whether treatment with these agents affects noise-induced auditory thresholds *in vivo*.

Treatment with 3MA before TTS exposure converts TTS to PTS at both 16 and 32 kHz 14 days after the noise exposure. Under TTS-noise conditions, noise-induced auditory threshold shifts recover to baseline by 3 days after the exposure. However, treatment with the autophagy inhibitor 3MA prevented recovery of auditory thresholds to baseline and instead resulted in PTS with thresholds elevated about 25 dB at 16 kHz ($p=0.011$) and 40 dB at 32 kHz ($p<0.001$) (Fig. 9A). Moreover, TTS-noise exposure did not induce any OHC or IHC losses, while the addition of 3MA treatment resulted in the loss of OHCs in the basal region. All IHCs remained intact with or without 3MA treatment (Fig. 9B). Quantification of OHC losses along the entire length of the cochlear sensory epithelium showed that treatment with 3MA induced OHC loss following a base-to-apex gradient after TTS-noise exposure. OHC loss increased progressively from 20% at 4.5 mm ($t_7=3.895$, $p=0.006$), to 30% at 5 mm ($t_7=5.657$, $p<0.001$), and to 40% at 5.5 mm from the apex ($t_7=6.477$, $p<0.001$) (Fig. 9C). Furthermore, 3MA treatment also significantly increased auditory threshold shifts at 16 kHz ($t_{10}=4.025$, $p=0.009$) and 32 kHz ($t_{10}=3.536$, $p=0.017$) 14 days after PTS-noise exposure (Fig. 9D).

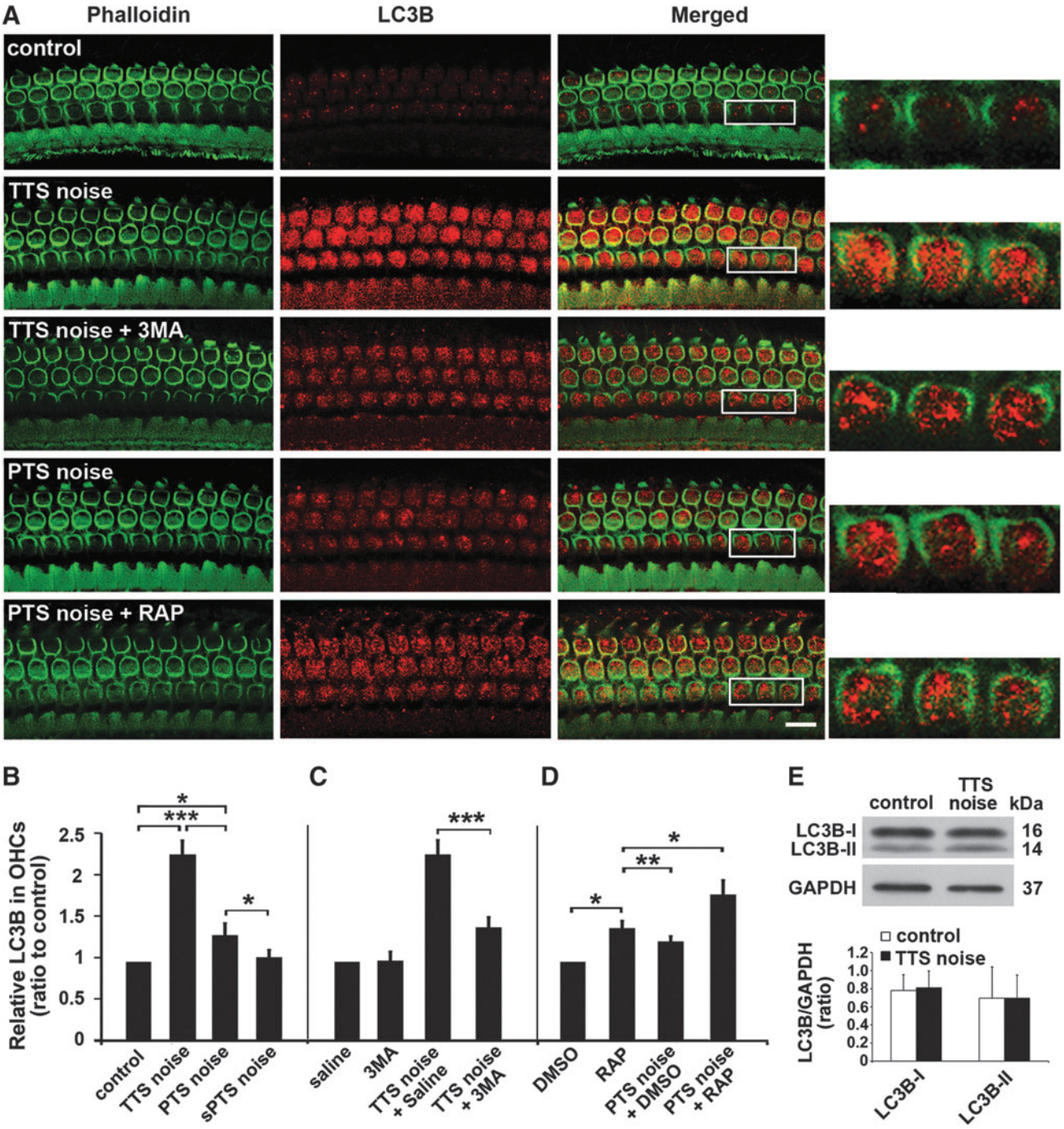

FIG. 4. Noise exposure and pharmacological autophagy regulators alter the levels of LC3B in OHCs. (A) Representative images of immunolabeled LC3B (*red*) in OHCs with phalloidin staining (*green*) 1 h after TTS noise with or without 3MA and 1 h after PTS noise with or without rapamycin compared with control mice without noise exposure. Enlarged images of the three OHCs outlined by *white rectangles* illustrate punctuate labeling. Images were taken from the basal turn. $n \geq 3$. Scale bar = 10 μm. **(B)** Quantification of LC3B immunolabeling in OHCs under the three noise conditions revealed a significant increase 1 h after TTS and PTS noise, but not after sPTS noise exposure, with significantly stronger immunolabeling in TTS than PTS. **(C)** Treatment with the autophagy inhibitor 3MA significantly decreased TTS-noise-induced LC3B immunofluorescence in OHCs. **(D)** Treatment with the autophagy activator rapamycin significantly increased PTS-noise-induced LC3B immunofluorescence in OHCs. Data **(B–E)** are presented as means + SD. $n = 3$ for both the 3MA and DMSO groups, $n = 4$ for the control, saline, RAP, TTS, TTS + saline, and sPTS groups, $n = 5$ for PTS and TTS + 3 MA, $n = 9$ for PTS + RAP; $^{*}p < 0.05$, $^{**}p < 0.01$, $^{***}p < 0.001$. **(E)** Western blotting using total cochlear homogenates shows both LC3B I and II bands with no difference between TTS and controls. GAPDH served as the sample loading control. $n = 3$. 3MA, 3-methyladenine; DMSO, dimethyl sulfoxide; LC3B: microtubule-associated protein light chain 3 B; RAP, rapamycin. To see this illustration in color, the reader is referred to the web version of this article at www.liebertpub.com/ars

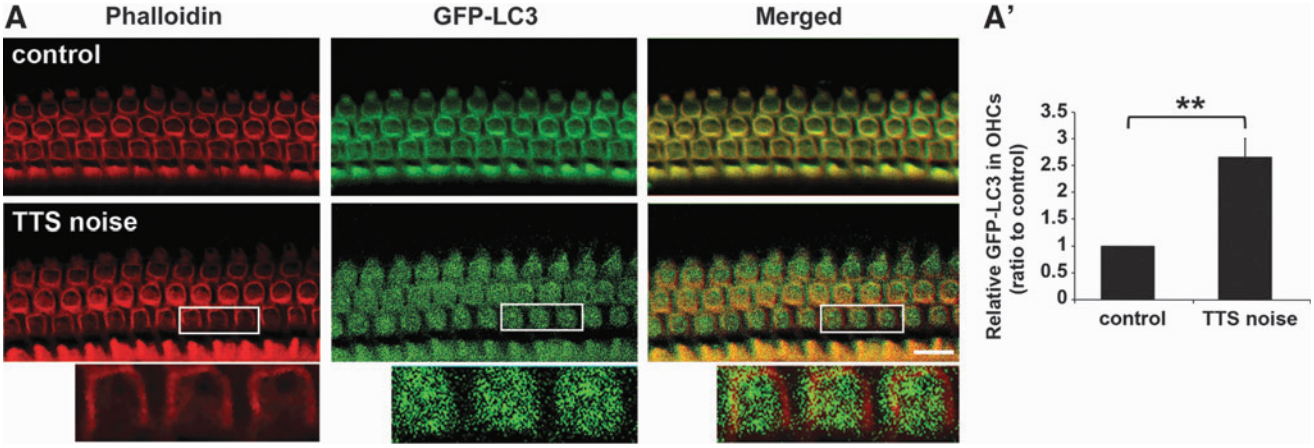

FIG. 5. GFP-LC3 transgene mice show an increase in GFP fluorescence 1 h after TTS-noise exposure. (A) Representative images of GFP-LC3 transgene mice with or without TTS-noise exposure. Enlarged images of the three OHCs outlined by *white rectangles* illustrate puctuate fluorescence. *Red*: Alexa-Fluor-594-phalloidin labeling of OHCs. Images were taken from the basal turn, scale bar = 10 μm. **(A′)** Quantification of GFP-LC3 *green* fluorescence in OHCs revealed a significant increase after TTS-noise exposure. Data are presented as means + SD. $n = 4$. $^{**}p < 0.01$. GFP, green fluorescent protein. To see this illustration in color, the reader is referred to the web version of this article at www.liebertpub.com/ars

Similarly, the depression of LC3B levels by pretreatment with siLC3B exacerbated NIHL under PTS noise conditions (Fig. 9E). Auditory threshold shifts of siLC3B-treated groups (PTS noise, PTS noise + siControl, PTS noise + siLC3B) were significantly different at both 16 kHz ($F_{2,30} = 5.23$, $p = 0.012$) and 32 kHz ($F_{2,30} = 3.801$, $p = 0.035$), but not at 8 kHz ($F_{2,30} = 0.308$, $p = 0.688$). The threshold shifts of siLC3B-pretreated mice significantly increased by about 15 dB at 16 kHz ($p = 0.033$) and marginally increased at 32 kHz ($p = 0.058$) compared with siControl treatment.

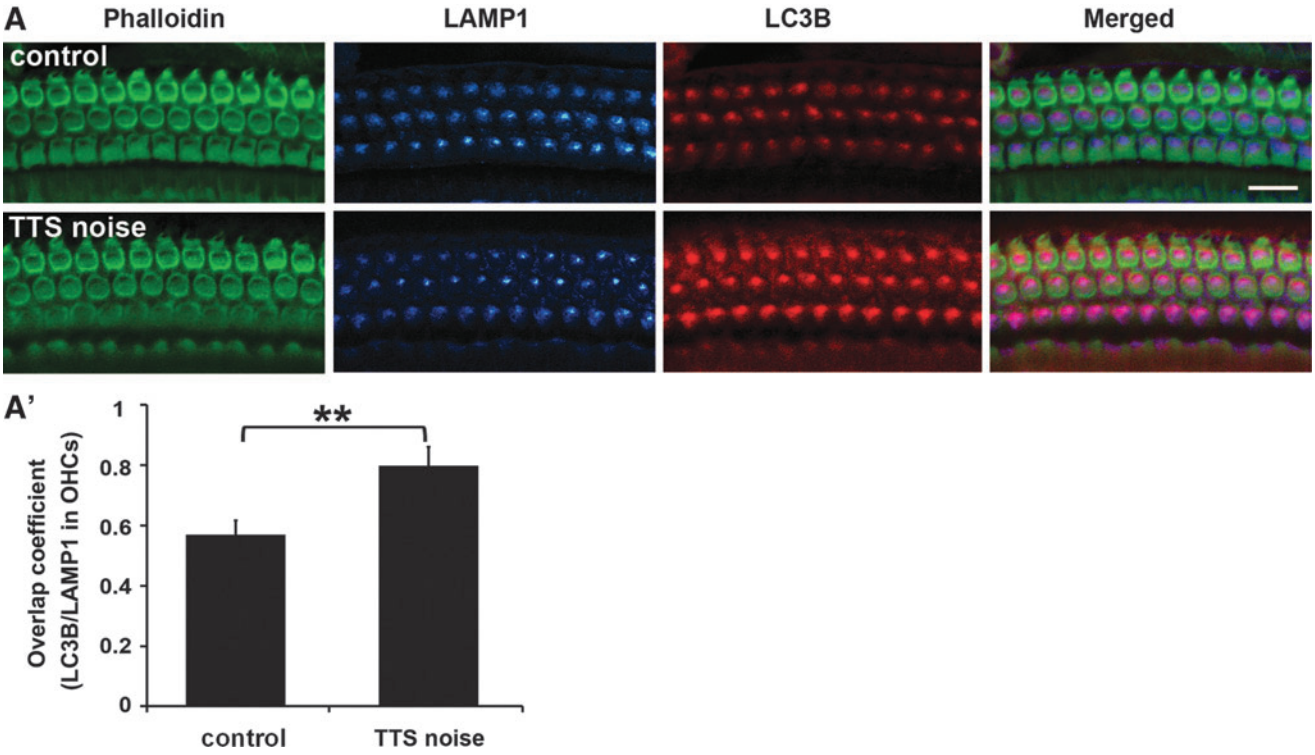

FIG. 6. Exposure to TTS increases the formation of LC3B/LAMP1 autophagic lysosomal complexes. (A) Surface preparations illustrate the immunolabeling for the lysosomal marker LAMP1 (*blue*), the autophagy marker LC3B (*red*) in OHCs with phalloidin staining (*green*), and the co-localization (*pink*) of LC3B- and LAMP1-associated immunofluorescence within OHCs (*merged*). All representative images were taken from the basal turn. $n = 6$. Scale bar = 10 μm. **(A′)** Quantification of the overlap coefficient for LC3B/LAMP1 immunolabeling in OHCs 1 h after TTS-noise exposure revealed a significant increase in autolysosome complexes. Data are presented as means + SD. $n = 6$. $^{**}p < 0.01$. To see this illustration in color, the reader is referred to the web version of this article at www.liebertpub.com/ars

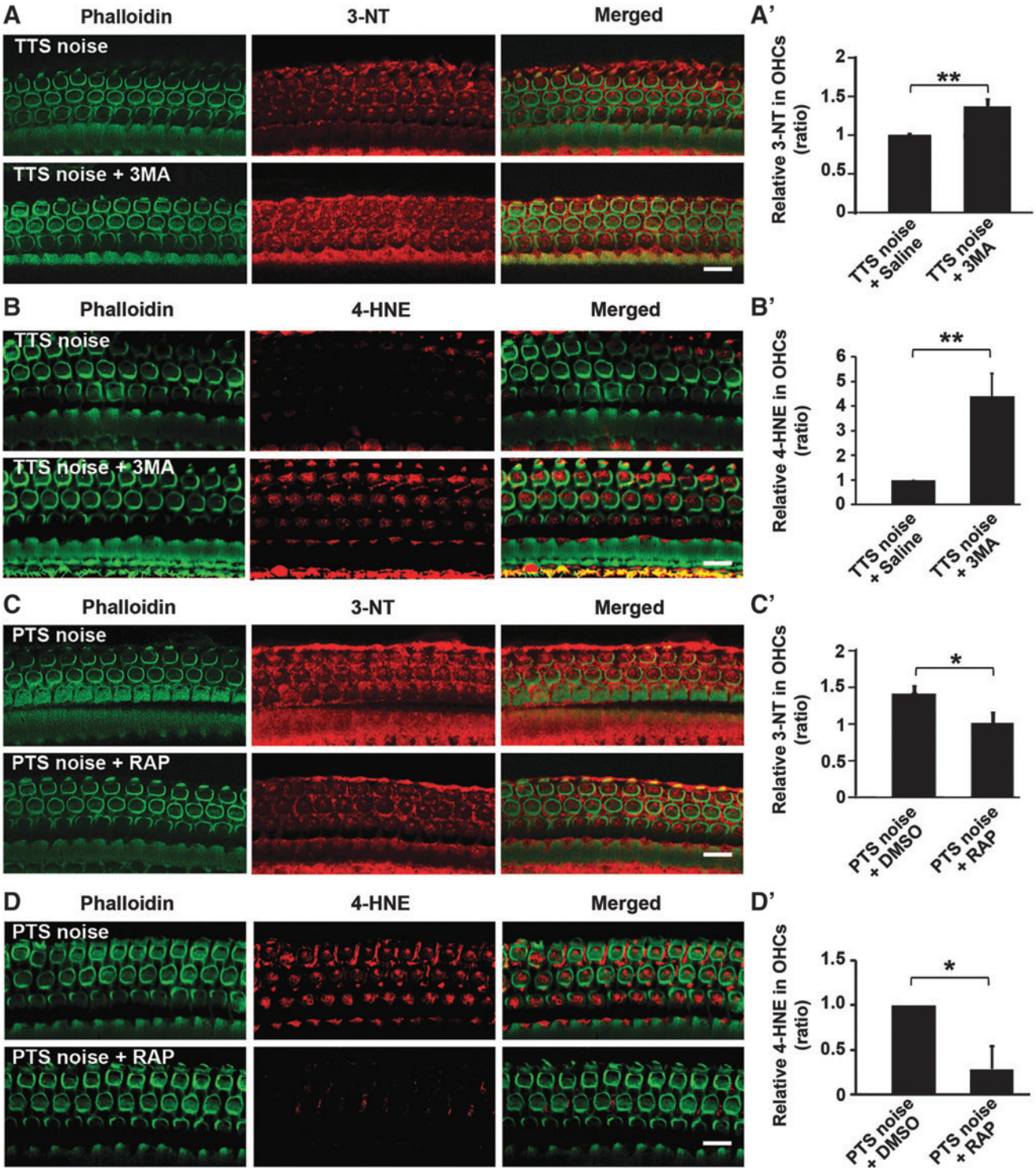

FIG. 7. Pharmacological modulation of autophagy alters the expression of 3-NT and 4-HNE in OHCs. **(A)** Immunolabeled 3-NT (*red*) in OHCs with phalloidin labeling (*green*) was greater with 3MA treatment 1 h after TTS-noise exposure. $n = 3$. **(A′)** Treatment with 3MA increases TTS-noise-induced 3-NT levels in OHCs. $n = 3$. **(B)** Immunolabeled 4-HNE (*red*) in OHCs with phalloidin staining (*green*) was stronger with 3MA 1 h after TTS-noise exposure. $n = 3$. **(B′)** Treatment with 3MA increased TTS-noise-induced 4-HNE levels in OHCs. $n = 3$. **(C)** Immunolabeled 3-NT (*red*) in OHCs with phalloidin staining (*green*) 1 h after PTS-noise was weaker with rapamycin treatment. $n = 6$. **(C′)** Treatment with rapamycin diminished PTS-noise-induced 3-NT levels in OHCs. $n = 6$. **(D)** Immunolabeled 4-HNE (*red*) in OHCs with phalloidin staining (*green*) 1 h after PTS noise decreased with rapamycin. $n = 4$. **(D′)** Treatment with rapamycin reduced the PTS-noise-induced increases in 4-HNE levels in OHCs. $n = 4$. Representative images **(A–D)** were taken from the basal turn. Scale bar = 10 μm. Data **(A′–D′)** are presented as means + SD. $^{*}p < 0.05$, $^{**}p < 0.01$. To see this illustration in color, the reader is referred to the web version of this article at www.liebertpub.com/ars

Remarkably, pretreatment with siLC3B escalated threshold shifts from TTS to PTS at 32 kHz. Auditory threshold shifts of the four groups (control, TTS noise, TTS + siControl, TTS + siLC3B) were significantly different at 32 kHz ($F_{3,18} = 10.548$, $p < 0.001$). Pretreatment with siLC3B increased auditory threshold shifts to 15 dB at 2 weeks after TTS-noise exposure ($p = 0.001$) (Fig. 9F).

In contrast to the earlier results, treatment with the autophagy inducer rapamycin significantly reduced PTS-noise-induced auditory threshold shifts at both 16 ($F_{2,31} = 33.538$, $p < 0.001$) and 32 kHz ($F_{3,48} = 23.895$, $p < 0.001$), but not at 8 kHz 2 weeks after noise exposure compared with vehicle (DMSO)-treated groups. Treatment with rapamycin reduced auditory threshold shifts at 16 kHz by 15 dB ($p < 0.01$) and 10 dB at 32 kHz ($p < 0.01$) (Fig. 9G). Meanwhile, rapamycin treatment also reduced PTS-noise-induced OHC losses (Fig. 9H). Quantification of OHC loss along the length of cochlear epithelium revealed significant reduction with addition of rapamycin treatment ($F_{1,13} = 39.321$, $p < 0.001$) (Fig. 9I). OHC loss was reduced by 15% at 3.5 mm ($p = 0.045$), 20% at 4 mm ($p < 0.001$), 25% at 4.5 mm ($p < 0.001$), and 10% at 5 mm ($p = 0.001$) from the apex. In addition, rapamycin treatment accelerated hearing recovery from TTS-noise exposure at both 16 kHz ($F_{2,9} = 16.35$, $p = 0.001$) and 32 kHz ($F_{2,9} = 15.269$, $p = 0.001$) (Fig. 9J). TTS-noise-induced auditory threshold shifts returned to baseline within 2 days with rapamycin treatment instead of 3 days, as for controls. The auditory threshold shifts were reduced by 30 dB at 16 kHz on day 1 ($p = 0.003$) and 15 dB at 32 kHz on day 1 ($p = 0.008$) and by 25 dB on day 2 ($p < 0.001$) after noise exposure.

Discussion

The salient finding of this study is that oxidative stress, as indicated by products of lipid oxidation (4-HNE) and protein nitration (3-NT) levels, is significantly elevated in a noise-dose-dependent fashion, whereas autophagy (based on LC3B levels) is significantly increased after TTS-, mildly increased after PTS-, and at control levels after sPTS-noise exposure. Thus, activation of autophagy appears to decrease noise-induced OHC death and NIHL by attenuating oxidative stress. Specifically, induction of autophagy by rapamycin reduces noise-induced oxidative stress (as measured by 4-HNE and 3-NT) and subsequent NIHL. Conversely, reduction of autophagy with the inhibitor 3MA or through pretreatment with siLC3B leads to increased levels of 3-NT and 4-HNE, exacerbating NIHL and hair cell death.

The findings in this mouse model that we have extensively characterized here are consistent with an earlier report using rats, in which hearing loss and the magnitude of cochlear lesions correlate with the intensity of noise exposure (8). OHCs play a significant role in auditory performance *via* their activity as motor units that amplify movements of the basilar membrane in response to sound stimuli. OHCs are more susceptible to noise trauma than IHCs. The correlation of NIHL and OHC loss was seen in the basal regions of the cochlea, but not in the apical regions. This partial correlation is in good agreement with previous reports (3, 8). Based on the frequency maps of Müller (34), the area coding to 8 kHz is located around 1 mm from the apex of cochlear sensory epithelium. However, roughly 40-dB threshold shifts at 8 kHz occur under sPTS-noise conditions (106 dB SPL) without OHC losses in that region. This may be due, in part, to surviving hair cells with damaged stereocilia, since the process of mechanical transduction occurs at the tips of these stereocilia (17). In addition, we found that young adult mice were more sensitive than mature adult mice to noise damage, as 96 dB SPL induces TTS in 3-month-old CBA/J mice, while only 90 dB SPL is required to produce TTS in 5-week-old C57/B6 GFP-LC3 mice, in agreement with the report by Ohlemiller and colleagues (36).

Noise-induced oxidative stress, as indicated by products of lipid oxidation (4-HNE) and protein nitration (3-NT) in cochlear tissues, including OHCs, is well documented (35, 52, 53). The results presented here are consistent with the literature demonstrating that noise exposure results in oxidative stress, as detected by the elevated protein nitration levels of 3-NT both in OHCs and in whole cochlear tissue homogenates, and by the elevated products of lipid oxidation 4-HNE levels in OHCs, but not in the cochlear tissue homogenates. The discrepancy in 4-HNE levels between the immunolabeled OHCs and immunoblots using whole cochlear tissue homogenates is intrinsic to such studies due to the fact that multiple cell types, including spiral ganglion, stria vascularis, and supporting cells are included in the homogenates, masking changes occurring only in OHCs. Increases in 3-NT and 4-HNE levels in OHCs are noise-dose dependent, providing further support for the concept of oxidative damage inciting hair cell death and NIHL (10, 16, 38). Interestingly, the increased levels of 3-NT and 4-HNE in Deiters cells after noise exposure in the absence of supporting cell death observed in this study has been previously reported in animal models such as guinea pigs (53). The potential effects, if any, of oxidative damage after noise exposure in Deiters cells are

FIG. 8. Silencing LC3B decreases TTS-noise-enhanced LC3B elevation, but it increases the levels of 3-NT and 4-HNE in OHCs. (A) Pretreatment with LC3B siRNA resulted in decreases in immunolabeled LC3B (*red*) in OHCs with phalloidin staining (*green*) in unexposed mice 72 h after silencing. $n = 3$. **(A′)** Pretreatment with siLC3B caused a significant decrease in LC3B levels in OHCs. $n = 3$. **(B)** Immunolabeling with LC3B (*red*) in OHCs with phalloidin staining (*green*) after pretreatment with siLC3B revealed a decrease in LC3B expression in OHCs 1 h after TTS-noise exposure compared with siControl-treated mice. $n = 6$. **(B′)** Quantification of LC3B immuolabeling in OHCs confirmed a significant decrease with siLC3B pretreatment. $n = 6$. **(C)** Immunolabeled 3-NT (*red*) in OHCs with phalloidin staining (*green*) was stronger 1 h after TTS exposure in cochleae with siLC3B pretreatment compared with those of siControls. $n = 5$. **(C′)** Quantification of 3-NT immunolabeling in OHCs confirmed a significant increase with pretreatment of LC3B siRNA. $n = 5$. **(D)** Immunolabeled 4-HNE (*red*) in OHCs with phalloidin staining (*green*) was stronger 1 h after TTS-noise exposure in cochleae with pretreatment with siLC3B compared with those of siControls. $n = 3$. **(D′)** Quantification of 4-HNE-immunolabeling in OHCs confirmed a significant increase with pretreatment with LC3B siRNA. Representative images **(A–D)** were taken from the basal turn. Scale bar = 10 μm. Data **(A′–D′)** are presented as means + SD. *$p < 0.05$, **$p < 0.01$. siControl, scrambled siRNA; siLC3B, LC3B siRNA. To see this illustration in color, the reader is referred to the web version of this article at www.liebertpub.com/ars

not known, but the protection of hair cells from aminoglycoside treatment by secretion of HSP70 from supporting cells has been recently reported (27).

The formation of ROS, such as superoxide, hydroxyl radicals, and nitric oxide, may occur by different mechanisms depending on the stress. The precise origin of ROS in the cochlea after noise exposure remains speculative. Several sources are likely to contribute. A surge of superoxide radicals followed by chain reaction formation of other free radicals (*via* Fenton-type reactions) may be due to increased mitochondrial activity, prolonged tissue hypoxia due to vasoconstriction (29), and rebound hyperperfusion (46). RNS may also arise from the activation or induction of the enzyme nitric oxide synthase. When produced in excess, not only is

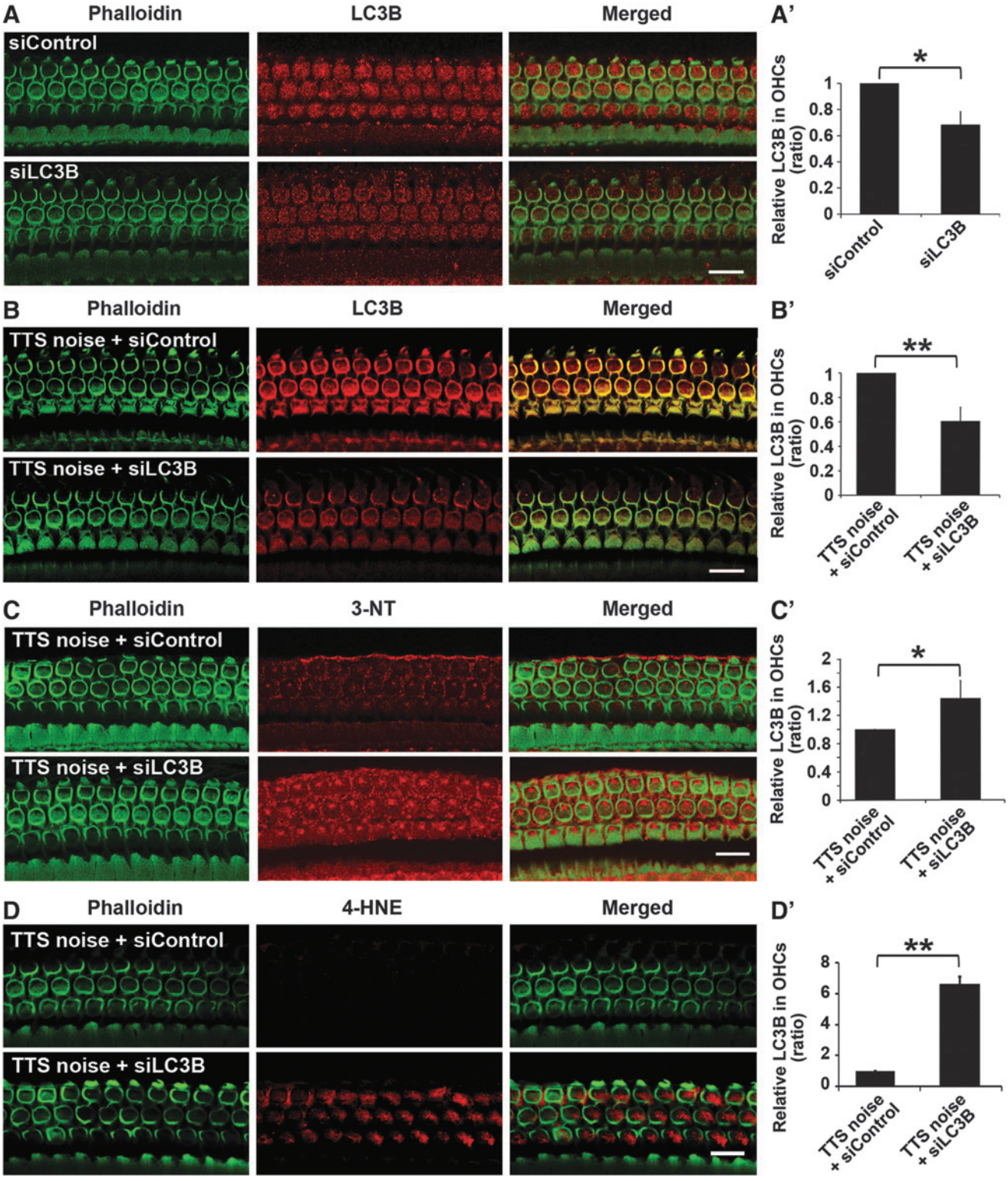

nitric oxide potentially damaging as a free radical, but it can also combine with superoxide to produce peroxynitrite, which is one of the more reactive and destructive free radicals. Nitric oxide levels can rise after noise exposure (44, 53), perhaps as a consequence of an enhanced release of excitatory amino acids (39, 40), and may contribute to the overall pathophysiology of noise-induced hair cell loss.

In contrast, the levels of LC3B in OHCs are markedly higher under TTS-noise conditions and unaltered with greater noise intensity (sPTS). The opposing behaviors of autophagy (LC3B) and oxidative stress, as indicated by products of lipid oxidation (4-HNE) and protein nitration (3-NT) under these noise conditions, suggest that a balance between oxidative stress and autophagy exists in sensory hair cells. The enhanced co-localization of LC3B with the lysosomal marker LAMP1 in OHCs under TTS-noise conditions demonstrates the fusion of autophagosomes and lysosomes to form autolysosomes, presumably to mediate the degradation of cellular constituents damaged by oxidative stress. We can conclude from these results that exposure to TTS noise induces low levels of oxidative stress and activates the autophagy process, whereas sPTS noise induces excessive oxidative stress resulting in oxidative damage.

Another line of evidence supporting the earlier conclusions comes from the pharmacological manipulation of autophagy in OHCs and pretreatment of LC3B siRNA in CBA/J mice. The autophagy-inducer rapamycin enhances the levels of LC3B and blocks PTS-noise-induced 3-NT and 4-HNE formation, while the autophagy inhibitor 3MA enhances noise-induced 3-NT and 4-HNE formation and diminishes LC3B. In addition, silencing of LC3B produces the same effects as 3MA pretreatment, further substantiating the idea that autophagy inhibits oxidative stress incurred during noise stress. These data are compatible with the general concept that small to moderate amounts of ROS promote autophagy to recycle damaged cellular constituents and maintain cellular homeostasis (2). Furthermore, activation of autophagy contributes to survival of spiral ganglion neurons in the cochlea of young SAMP9 mice, but promotes cell death in spiral ganglia of older animals (28). In addition, the early upregulation of autophagy protects against brain injury by removing damaged mitochondria (22). Since we predict that noise-induced oxidative stress may originate from mitochondria, mitophagy, the targeted lysosomal degradation of mitochondria, might also play a relevant role in maintaining the balance between the generation of ROS and antioxidant detoxification. This speculation deserves investigation in future studies.

Numerous genetic and biochemical studies have shown that mTORC1 negatively regulates autophagy (30). Treatment with rapamycin induces LC3B expression, in line with the concept that rapamycin can induce autophagy by blocking activation of the mTORC1 pathway (5, 49). However, the two pharmacological manipulators used in this study to modulate autophagy, rapamycin and 3MA, may have other pharmacological effects on the cells in addition to their effect on autophagy. For example, protection against NIHL by rapamycin may be only partly due to its effects on autophagy since rapamycin treatment also regulates other signaling molecules in OHCs. We speculate that rapamycin may stimulate Akt pro-survival signaling pathways in OHCs that attenuate PTS, as rapamycin treatment is known to promote Akt activation (5, 15, 47). In contrast, decreased levels of Akt pro-survival molecules in OHCs are found in aminoglycoside-induced hearing loss and age-related hearing loss (9, 19, 20, 43). In addition, inhibition of the TOR signaling pathway by feeding mice rapamycin extends their lifespan (14). On the other hand, the similar effect of the two different compounds (with different secondary actions) supports our contention of autophagy as a common target.

In summary, this study demonstrates that the oxidative stress, as indicated by products of lipid oxidation (4-HNE) and protein nitration (3-NT) in OHCs, is noise-dose dependent. The low levels of oxidative stress induced by TTS noise increased LC3B in OHCs, blocking noise-induced oxidative damage. In contrast, the overproduction of 3-NT and 4-HNE by PTS noise resulted in oxidative damage. Treatment with rapamycin increased LC3B levels in OHCs by blocking mTORC1, reducing the amount of 3-NT, and preventing NIHL and hair cell death. On the other hand, reduction of LC3B by the autophagy inhibitor 3MA or LC3B siRNA increased the levels of 3-NT in OHCs and promoted noise-induced hair cell loss and NIHL (Fig. 10). Our results suggest that autophagy is an intrinsic cellular process that protects against NIHL by attenuating oxidative stress. Furthermore, these novel observations suggest an untried yet potentially valuable approach to the amelioration of NIHL by activation of autophagy.

FIG. 9. Autophagy regulators modulate NIHL. (A) Treatment with 3MA before TTS exposure converts TTS to PTS at both 16 and 32 kHz 14 days after the exposure. Control and 3MA groups: $n=6$, TTS: $n=7$, TTS noise + 3MA: $n=8$. **(B)** Representative images were taken in the region 4.5 mm from the apex of the cochlear epithelium 14 days after TTS exposure. OHCs are intact in TTS-exposed mice, but missing with TTS noise + 3MA treatment. OHC 1, 2, and 3 indicate OHC rows 1, 2, and 3; IHC indicates the one row of IHCs. $n=7$. Scale bar = 10 μm. **(C)** Quantitative analysis of OHCs revealed significant loss of OHCs after TTS-noise exposure with 3MA treatment. TTS noise only: $n=7$, TTS noise + 3MA treatment: $n=8$. **(D)** 3MA treatment potentiates PTS-noise-induced threshold shifts 14 d after PTS exposure. control: $n=6$, 3MA: $n=6$, PTS noise: $n=9$, PTS noise + 3MA: $n=3$. **(E)** LC3B siRNA enhances PTS-noise-induced auditory threshold shifts at 16 kHz 14 days after exposure compared with mice treated with control siRNA. $n=6$ for both control and PTS noise + siLC3B, $n=7$ for PTS noise + siControl, $n=18$ for PTS noise. **(F)** TTS-noise-induced threshold shifts persist and become PTS at 32 kHz with pretreatment with LC3B siRNA 14 days after noise exposure. $n=6$. **(G)** Rapamycin treatment reduced PTS-noise-induced threshold shifts at both 16 and 32 kHz 14 days after noise exposure. PTS noise only: $n=12$, PTS noise + RAP: $n=14$, control and PTS noise + vehicle groups: $n=6$. RAP indicates rapamycin. **(H)** Representative images were taken in the region 4.0 mm from the apex of the cochlear epithelium 14 days after noise exposure. Rapamycin treatment resulted in less OHC loss. $n=7$. Scale bar = 10 μm. **(I)** The percentage of OHC loss was significantly lower in the PTS-noise-plus-rapamycin group compared with PTS noise plus vehicle only. PTS noise + vehicle: $n=7$, PTS + RAP: $n=8$, control group: $n=6$. **(J)** Rapamycin treatment also accelerated TTS recovery. Auditory threshold shifts at both 16 and 32 kHz were significantly reduced by days 1 and 2 after TTS-noise exposure. Data **(A, C, D, F, G, I, J)** are presented as means + SD, $*p<0.05$, $**p<0.01$, $***p<0.001$. NIHL, noise-induced hearing loss.

Materials and Methods

Animals

Male CBA/J mice at the age of 11 weeks (Harlan Sprague – Dawley, Indianapolis, IN) or male C57BL6 GFP-LC3 mice (23, 31) at 5 weeks of age (kindly provided by Dr. John Lemasters at MUSC) had free access to water and a regular mouse diet (Purina 5025; Purina, St. Louis, MO) and were kept at 22°C ± 1°C under a standard 12:12 h light-dark cycle to acclimate for 1 week before the experiments. All animal

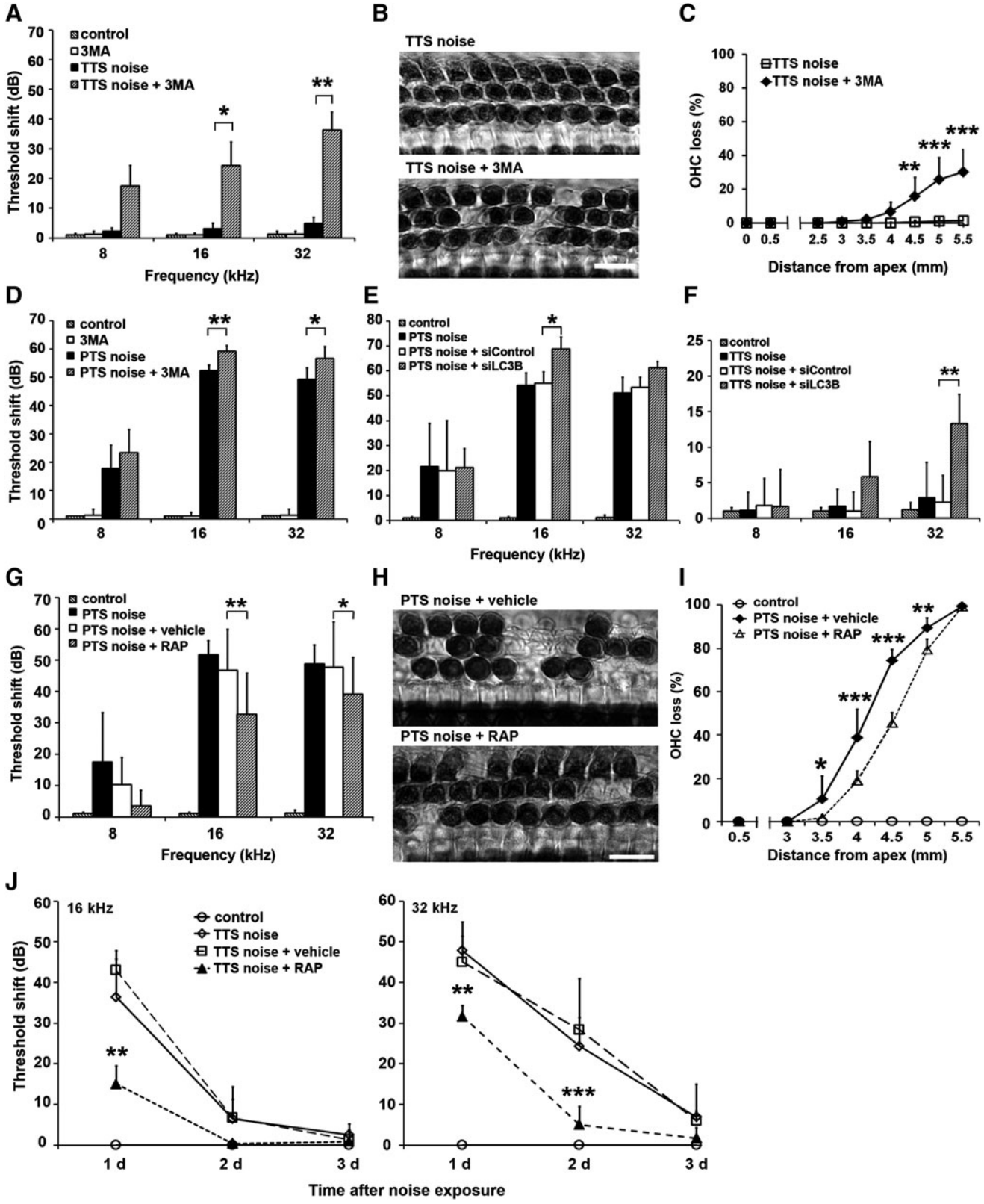

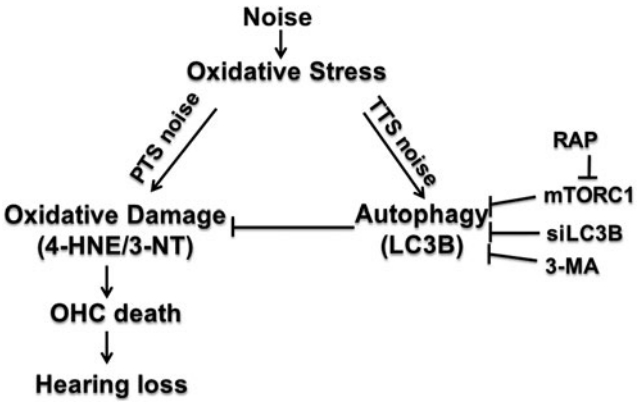

FIG. 10. Summary. The levels of oxidative stress, as indicated by products of lipid oxidation (4-HNE) and protein nitration (3-NT) in OHCs, differ significantly after TTS and PTS noise. TTS noise induces lower levels of oxidative stress and an increase in autophagy (LC3B) in OHCs, which results only in temporary hearing loss without death of OHCs. In contrast, the PTS-noise-induced overproduction of 3-NT and 4-HNE leads to hair cell death *via* oxidative damage. Elevation of LC3B by administration of an LC3B inducer (rapamycin) blocks the expression of 3-NT and 4-HNE and prevents NIHL. On the other hand, reduction of LC3B by LC3B inhibitors, that is, 3MA or LC3B siRNA, increases the levels of 3-NT and 4-HNE in OHCs and promotes noise-induced hair cell loss and, subsequently, NIHL.

experiments were approved by the Institutional Animal Care and Use Committee (IACUC) at the Medical University of South Carolina (MUSC). Animal care was under the supervision of the Division of Laboratory Animal Resources at MUSC.

Noise exposure

Mice were exposed in the same sound chamber as previously reported (6, 54). Briefly, unrestrained CBA/J mice at the age of 12 weeks were exposed to BBN with a frequency spectrum from 2 to 20 kHz for 2 h at 106-dB SPL to induce sPTS, 98-dB SPL to induce PTS, and 96-dB SPL to induce TTS. C57BL6 GFP-LC3 mice at 5 weeks of age were exposed to 90-dB SPL to induce TTS, since young adult mice are more sensitive to noise damage than older mice (36). As C57BL6 mice carry two copies of the age-related hearing loss gene (*Ahl*), and begin to lose high-frequency hearing at 2 months of age (13, 24), we used GFP-LC3 mice at the age of 5 weeks to avoid such a confounding factor.

Based on our previous studies, we focused on the molecular events of autophagy (using LC3B as a marker) and oxidative stress (3-NT and 4-HNE as markers) in OHCs using immunolabeling on surface preparations at the time point of 1 h after noise exposure (6).

Auditory brainstem responses

We followed the ABR measurement procedure that has been previously described in detail (6, 54). Thresholds were estimated between the lowest stimulus level where a response was observed and the highest level without response. All ABR measurements were conducted by the same experimenter. The ABR scores were assigned by an expert who was blinded to the treatment conditions.

Drug administration via *intra-peritoneal route*

Rapamycin (LC Laboratories, Woburn, MA) was dissolved in DMSO as a stock solution (75 mg/ml) and stored at − 20°C. 3MA (Sigma-Aldrich, St. Louis, MO) was dissolved in 0.9% saline as a stock solution (30 mg/ml) and stored at − 20°C. The solution was heated to 60°C to completely dissolve the 3MA and then allowed to cool at room temperature before being used for injections. NAC was dissolved in 0.2 *M* sodium hydroxide (NaOH) as a stock solution (650 mg/ml) and stored at − 20°C. The stock solutions of rapamycin and 3MA were diluted with saline, and NAC was diluted with 0.2 *M* NaOH immediately before being injected into animals. Each animal received a total of three intra-peritoneal (IP) injections of rapamycin at a dose of 7.5 mg/kg per injection, 3MA at a dose of 30 mg/kg per injection, or NAC at a dose of 325 mg/kg based on conditions reported in the literature (21, 25, 42). IP injections were administered 24 h before, 2 h before, and immediately after noise exposure. The animals were euthanized 1 h after noise exposure and the temporal bones were removed to dissect the cochleae for immunofluorescence assays. The mice used for the experiments designed to observe the evolution of ABR thresholds after noise exposure received a fourth IP injection 24 h after noise exposure.

Intratympanic delivery of siRNA

siLC3B (Invitrogen, Carlsbad, CA) or siControl (Invitrogen) was locally delivered *via* intra-tympanic application. We followed the procedures as previously described (7, 37).

Two concentrations of siLC3B, 0.6 and 0.3 μg, were tested for preliminary study, and 0.6 μg of siLC3B or siControl was selected due to relative high efficiency for the described experimental studies.

Immunocytochemistry for cochlear surface preparations and quantification of the immunofluorescence signals from surface preparations

The detailed procedures of immunocytochemistry for cochlear surface preparations and quantification of the immunolabeling signals in OHCs were described in our previous reports (6, 54). The concentrations of primary antibodies used in these studies were polyclonal rabbit anti-LC3B at 1:50 (Cell Signaling Technology, Danvers, MA), polyclonal rabbit anti-nitrotyrosine at 1:50 (EMD Millipore, Billerica, MA), and polyclonal rabbit anti-4-HNE at 1:50 (Abcam, Inc., Cambridge, MA). Alexa-Fluor-594- or 350-conjugated secondary antibodies were at a concentration of 1:200, and Alexa Fluor 488 phalloidin was at a concentration of 1:100 (Life Technologies, Grand Island, NY). For the co-localization of LC3B and LAMP1, the specimens were first incubated with primary monoclonal mouse anti-MAP LC3B (G-2) (Santa Cruz Biotechnology, Dallas, TX) at 1:50 and the secondary antibody and then with primary rabbit anti-LAMP1 antibody at 1:50 (Sigma-Aldrich) and the secondary antibody.

The immunolabeling of LC3B, 3-NT, and 4-HNE was quantified from original confocal images, each taken with a

63×-magnification lens under identical conditions and equal parameter settings for laser gains and photomultiplier tube gains, using ImageJ software (National Institutes of Health, Bethesda, MD). The cochleae from the different groups were fixed, labeled simultaneously with identical solutions, and processed in parallel. All of the surface preparations were counter-labeled with Alexa-Fluor-488 phalloidin (green) to label hair cell structure to identify the comparable parts of the OHCs in confocal images. The relative fluorescence was quantified by normalizing the ratio of average fluorescence of noise-exposed OHCs to the average fluorescence of the unexposed OHCs.

Surface preparations and diaminobenzidine staining of cochlear epithelia for hair cell counts

We followed the detailed procedures for surface preparations and diaminobenzidine (DAB) staining of myosin VII-labeled cochlear sensory epithelia for hair cell counts described in our previous reports (6, 54).

Extraction of total cochlear proteins for Western blot analysis

The detailed procedures for extraction of total cochlear protein for Western blot and quantification of the band densities were described in our previous publication (6, 54). Tissues from the cochleae of an individual mouse were homogenized in ice-cold RIPA lysis buffer (Sigma-Aldrich) plus Phosphatase Inhibitor Cocktails II and III (Sigma-Aldrich) and Roche Protease Inhibitor (Roche Diagnostic, Indianapolis, IN). The concentrations of primary antibodies were anti-LC3B (1:1000), anti-3-NT (1:1000), anti-4-HNE (1:1000), or anti-GAPDH (1:10,000) (EMD Millipore, Billerica, MA).

X-ray films of Western blots were scanned and analyzed using Image J software. The band densities were first normalized to background. Next, the probing protein/GAPDH ratio was calculated from the band densities run on the same gel. Finally, the difference in the ratio of the control and experimental bands was analyzed for statistical significance.

Statistical analysis

Data were analyzed using IBM SPSS Statistics Premium V21 and GraphPad software for Windows. The group size (n) *in vivo* was determined by the variability of measurements and the magnitude of the differences between groups. Based on our previous and current preliminary studies, we determined that six to eight animals per group provide sufficient statistical power. Statistical methods used included one-way analysis of variance (ANOVA) with Tukey's multiple comparisons, repeated-measures ANOVA with *post-hoc* testing, unpaired t-tests, and one-sample t-tests. All tests were two tailed, and a p-value < 0.05 was considered statistically significant.

Acknowledgments

The research project described was supported by grant R01 DC009222 from the National Institute on Deafness and Other Communication Disorders, National Institutes of Health. This work was conducted in the MUSC WR Building in renovated space supported by grant C06 RR014516. Animals were housed in MUSC CRI animal facilities supported by grant C06 RR015455 from the Extramural Research Facilities Program of the National Center for Research Resources. The authors thank Drs. Jochen Schacht and Bradley Schulte for their valuable comments on this article. They also thank statistician Dr. Fu-Shing Lee for statistical analysis consultation on the results in this article.

Author Disclosure Statement

There are no conflicts of interest for any of the authors.

The data contained in this article have not been previously published.

All research protocols were approved by the Institutional Animal Care and Use Committee at the Medical University of South Carolina (MUSC). Animal care was under the supervision of the Division of Laboratory Animal Resources at MUSC.

All authors have reviewed the contents of this article, approve of its contents, and validate the accuracy of the data.

References

1. Barth S, Glick D, and Macleod KF. Autophagy: assays and artifacts. *J Pathol* 221: 117–124, 2010.
2. Berliocchi L, Russo R, Maiaru M, Levato A, Bagetta G, and Corasaniti MT. Autophagy impairment in a mouse model of neuropathic pain. *Mol Pain* 7: 83, 2011.
3. Borg E. Loss of hair cells and threshold sensitivity during prolonged noise exposure in normotensive albino rats. *Hear Res* 30: 119–126, 1987.
4. Boya P, González-Polo RA, Casares N, Perfettini J, Dessen P, Larochette N, *et al.* Inhibition of macroautophagy triggers apoptosis. *Mol Cell Biol* 25: 1025–1040, 2005.
5. Carracedo A, Ma L, Teruya-Feldstein J, Rojo F, Salmena L, Alimonti A, Egia A, Sasaki AT, Thomas G, Kozma SC, Papa A, Nardella C, Cantley LC, Baselga J, and Pandolfi PP. Inhibition of mTORC1 leads to MAPK pathway activation through a PI3K-dependent feedback loop in human cancer. *J Clin Invest* 118: 3065–3074, 2008.
6. Chen FQ, Zheng HW, Hill K, and Sha SH. Traumatic noise activates rho-family gtpases through transient cellular energy depletion. *J Neurosci* 32: 12421–12430, 2012.
7. Chen FQ, Zheng HW, Schacht J, and Sha SH. Mitochondrial peroxiredoxin 3 regulates sensory cell survival in the cochlea. *PLoS One* 8: e61999, 2013.
8. Chen GD and Fechter LD. The relationship between noise-induced hearing loss and hair cell loss in rats. *Hear Res* 177: 81–90, 2003.
9. Chung WH, Pak K, Lin B, Webster N, and Ryan AF. A PI3K pathway mediates hair cell survival and opposes gentamicin toxicity in neonatal rat organ of Corti. *J Assoc Res Otolaryngol* 7: 373–382, 2006.
10. Fetoni AR, De Bartolo P, Eramo SL, Rolesi R, Paciello F, Bergamini C, Fato R, Paludetti G, Petrosini L, and Troiani D. Noise-induced hearing loss (NIHL) as a target of oxidative stress-mediated damage: cochlear and cortical responses after an increase in antioxidant defense. *J Neurosci* 33: 4011–4023, 2013.
11. Fubini B and Hubbard A. Reactive oxygen species (ROS) and reactive nitrogen species (RNS) generation by silica in inflammation and fibrosis. *Free Radic Biol Med* 34: 1507–1516, 2003.
12. Glick D, Barth S, and Macleod KF. Autophagy: cellular and molecular mechanisms. *J Pathol* 221: 3–12, 2010.

13. Harding GW, Bohne BA, and Vos JD. The effect of an age-related hearing loss gene (Ahl) on noise-induced hearing loss and cochlear damage from low-frequency noise. *Hear Res* 204: 90–100, 2005.
14. Harrison DE, Strong R, Sharp ZD, Nelson JF, Astle CM, Flurkey K, Nadon NL, Wilkinson JE, Frenkel K, Carter CS, Pahor M, Javors MA, Fernandez E, and Miller RA. Rapamycin fed late in life extends lifespan in genetically heterogeneous mice. *Nature* 460: 392–395, 2009.
15. Harston RK, McKillop JC, Moschella PC, Van Laer A, Quinones LS, Baicu CF, Balasubramanian S, Zile MR, and Kuppuswamy D. Rapamycin treatment augments both protein ubiquitination and Akt activation in pressure-overloaded rat myocardium. *Am J Physiol Heart Circ Physiol* 300: H1696–H1706, 2011.
16. Henderson D, Bielefeld EC, Harris KC, and Hu BH. The role of oxidative stress in noise-induced hearing loss. *Ear Hear* 27: 1–19, 2006.
17. Hu BH, Zheng XY, McFadden SL, and Kopke RD, Henderson D. R-phenylisopropyladenosine attenuates noise-induced hearing loss in the chinchilla. *Hear Res* 113: 198–206, 1997.
18. Jamesdaniel S, Ding D, Kermany MH, Davidson BA, Knight PR, 3rd, Salvi R, and Coling DE. Proteomic analysis of the balance between survival and cell death responses in cisplatin-mediated ototoxicity. *J Proteome Res* 7: 3516–3524, 2008.
19. Jiang H, Sha SH, and Schacht J. NF-kappaB pathway protects cochlear hair cells from aminoglycoside-induced ototoxicity. *J Neurosci Res* 79: 644–651, 2005.
20. Jiang H, Sha SH, and Schacht J. Kanamycin alters cytoplasmic and nuclear phosphoinositide signaling in the organ of Corti *in vivo*. *J Neurochem* 99: 269–276, 2006.
21. Jiang M, Liu K, Luo J, and Dong Z. Autophagy is a renoprotective mechanism during *in vitro* hypoxia and *in vivo* ischemia-reperfusion injury. *Am J Pathol* 176: 1181–1192, 2010.
22. Jing CH, Wang L, Liu PP, Wu C, Ruan D, and Chen G. Autophagy activation is associated with neuroprotection against apoptosis via a mitochondrial pathway in a rat model of subarachnoid hemorrhage. *Neuroscience* 213: 144–153, 2012.
23. Kuma A and Mizushima N. Chromosomal mapping of the GFP-LC3 transgene in GFP-LC3 mice. *Autophagy* 4: 61–62, 2008.
24. Li HS and Borg E. Age-related loss of auditory sensitivity in two mouse genotypes. *Acta Otolaryngol* 111: 827–834, 1991.
25. Lu J, Li W, Du X, Ewert DL, West MB, Stewart C, Floyd RA, and Kopke RD. Antioxidants reduce cellular and functional changes induced by intense noise in the inner ear and cochlear nucleus. *J Assoc Res Otolaryngol* 15: 353–372, 2014.
26. Martinez MC and Andriantsitohaina R. Reactive nitrogen species: molecular mechanisms and potential significance in health and disease. *Antioxid Redox Signal* 11: 669–702, 2009.
27. May LA, Kramarenko, II, Brandon CS, Voelkel-Johnson C, Roy S, Truong K, Francis SP, Monzack EL, Lee FS, and Cunningham LL. Inner ear supporting cells protect hair cells by secreting HSP70. *J Clin Invest* 123: 3577–3587, 2013.
28. Menardo J, Tang Y, Ladrech S, Lenoir M, Casas F, Michel C, Bourien J, Ruel J, Rebillard G, Maurice T, Puel JL, and Wang J. Oxidative stress, inflammation, and autophagic stress as the key mechanisms of premature age-related hearing loss in SAMP8 mouse Cochlea. *Antioxid Redox Signal* 16: 263–274, 2012.
29. Miller JM, Brown JN, and Schacht J. 8-iso-prostaglandin F(2alpha), a product of noise exposure, reduces inner ear blood flow. *Audiol Neurootol* 8: 207–221, 2003.
30. Mizushima N. The role of the Atg1/ULK1 complex in autophagy regulation. *Curr Opin Cell Biol* 22: 132–139, 2010.
31. Mizushima N and Kuma A. Autophagosomes in GFP-LC3 Transgenic Mice. *Methods Mol Biol* 445: 119–124, 2008.
32. Mizushima N, Yamamoto A, Matsui M, Yoshimori T, and Ohsumi Y. *In vivo* analysis of autophagy in response to nutrient starvation using transgenic mice expressing a fluorescent autophagosome marker. *Mol Biol Cell* 15: 1101–1111, 2004.
33. Mizushima N, Yoshimori T, and Levine B. Methods in mammalian autophagy research. *Cell* 140: 313–326, 2010.
34. Muller M, von Hunerbein K, Hoidis S, and Smolders JW. A physiological place-frequency map of the cochlea in the CBA/J mouse. *Hear Res* 202: 63–73, 2005.
35. Ohlemiller KK, Wright JS, and Dugan LL. Early elevation of cochlear reactive oxygen species following noise exposure. *Audiol Neurootol* 4: 229–236, 1999.
36. Ohlemiller KK, Wright JS, and Heidbreder AF. Vulnerability to noise-induced hearing loss in 'middle-aged' and young adult mice: a dose-response approach in CBA, C57BL, and BALB inbred strains. *Hear Res* 149: 239–247, 2000.
37. Oishi N, Chen FQ, Zheng HW, and Sha SH. Intra-tympanic delivery of short interfering RNA into the adult mouse cochlea. *Hear Res* 296: 36–41, 2013.
38. Oishi N and Schacht J. Emerging treatments for noise-induced hearing loss. *Expert Opin Emerg Drugs* 16: 235–245, 2011.
39. Puel JL, d'Aldin CG, Saffiende S, Eybalin M, and Pujol R. Excitotoxicity and plasticity of IHC-auditory nerve contributes to both temporary and permanent threshold shift. In: *Scientific Basis of Noise-induced Hearing Loss*, edited by Axelsson A, Borchgrevink HM, Hamernik RP, Hellström PA, Henderson D, and Salvi RJ. New York: Thieme Press, 1996, pp. 36–42.
40. Puel JL, Pujol R, Tribillac F, Ladrech S, and Eybalin M. Excitatory amino acid antagonists protect cochlear auditory neurons from excitotoxicity. *J Comp Neurol* 341: 241–256, 1994.
41. Reggiori F and Klionsky DJ. Autophagy in the eukaryotic cell. *Eukaryot Cell* 1: 11–21, 2002.
42. Rodriguez-Muela N, Germain F, Marino G, Fitze PS, and Boya P. Autophagy promotes survival of retinal ganglion cells after optic nerve axotomy in mice. *Cell Death Differ* 19: 162–169, 2012.
43. Sha SH, Chen FQ, and Schacht J. PTEN attenuates PIP3/Akt signaling in the cochlea of the aging CBA/J mouse. *Hear Res* 264: 86–92, 2010.
44. Shi X, Ren T, and Nuttall AL. The electrochemical and fluorescence detection of nitric oxide in the cochlea and its increase following loud sound. *Hear Res* 164: 49–58, 2002.
45. Sies H. Oxidative stress: oxidants and antioxidants. *Exp Physiol* 82: 291–295, 1997.
46. Thorne PR, Nuttall AL, Scheibe F, and Miller JM. Sound-induced artifact in cochlear blood flow measurements using the laser Doppler flowmeter. *Hear Res* 31: 229–234, 1987.
47. Veilleux A, Houde VP, Bellmann K, and Marette A. Chronic inhibition of the mTORC1/S6K1 pathway increases insulin-induced PI3K activity but inhibits Akt2 and glucose transport stimulation in 3T3-L1 adipocytes. *Mol Endocrinol* 24: 766–778, 2010.
48. Vernon PJ and Tang D. Eat-me: autophagy, phagocytosis, and reactive oxygen species signaling. *Antioxid Redox Signal* 18: 677–691, 2013.

49. Vignot S, Faivre S, Aguirre D, and Raymond E. mTOR-targeted therapy of cancer with rapamycin derivatives. *Ann Oncol* 16: 525–537, 2005.
50. Wang CW and Klionsky DJ. The molecular mechanism of autophagy. *Mol Med* 9: 65–76, 2003.
51. Wang Z, Shi XY, Yin J, Zuo G, Zhang J, and Chen G. Role of autophagy in early brain injury after experimental subarachnoid hemorrhage. *J Mol Neurosci* 46: 192–202, 2012.
52. Yamane H, Nakai Y, Takayama M, Iguchi H, Nakagawa T, and Kojima A. Appearance of free radicals in the guinea pig inner ear after noise-induced acoustic trauma. *Eur Arch Otorhinolaryngol* 252: 504–508, 1995.
53. Yamashita D, Jiang HY, Schacht J, and Miller JM. Delayed production of free radicals following noise exposure. *Brain Res* 1019: 201–209, 2004.
54. Zheng H-W, Chen J, and Sha S-H. Receptor-interacting protein kinases modulate noise-induced sensory hair cell death. *Cell Death Dis* 5: e1262, 2014.

Address correspondence to:
Dr. Su-Hua Sha
Department of Pathology and Laboratory Medicine
Medical University of South Carolina
WRB/Room 403-E
39 Sabin St.
Charleston, SC 29425

E-mail: shasu@musc.edu

Date of first submission to ARS Central, May 27, 2014; date of final revised submission, January 13, 2015; date of acceptance, February 9, 2015.

Abbreviations Used

3MA = 3-methyladenine
3-NT = 3-nitrotyrosine
4-HNE = 4-hydroxynonenal
ABR = auditory brainstem response
BBN = broadband noise
DAB = diaminobenzidine
DMSO = dimethyl sulfoxide
GFP = green fluorescent protein
IHCs = inner hair cells
IP = intra-peritoneal
LC3B = microtubule-associated protein light chain 3 B
NAC = N-acetylcysteine
NIHL = noise-induced hearing loss
OHCs = outer hair cells
PTS = permanent threshold shift
RAP = rapamycin
RNS = reactive nitrogen species
ROS = reactive oxygen species
siControl = scrambled siRNA
siLC3B = LC3B siRNA
sPTS = severe PTS
TTS = temporary threshold shift